ADVANCED MATERIALS
www.advmat.de

Multi-Functional Lanthanide Metallopolymer: Self-Healing and Photo-Stimuli-Responsive Dual-Emitting Luminescence for Diverse Applications

Di Zhao, Lei Guo, Qianrui Li, Chunmei Yue, Bing Han, Kai Liu,* and Huanrong Li**

Photoluminescent metallopolymers displaying photo-stimuli-responsive properties are emerging as promising materials with versatile applications in photo-rewritable patterns, wearable UV sensors, and optical encryption anti-counterfeiting. However, integrating these materials into practical applications that require fast response times, lightweight qualities, fatigue resistance, and multiple encryption capabilities poses challenges. In this study, luminescent photochromic lanthanide (Ln) metallopolymers with rapid self-healing properties are developed by cross-linking terpyridine (Tpy)- and spiropyran (SP)- functionalized polyurethane chains through Ln-Tpy coordination bonds and H-bonds among polymer chains. The resulting products exhibit a range of intriguing features: i) photo-stimuli responsiveness using spiropyran monomers without additional dopants; ii) dual-emitting performance under UV-light due to Ln-Tpy and open-ring spiropyran moieties; iii) satisfactory mechanical properties and self-healing abilities from polymer chains; iv) multiple control switches for luminescence colors through photostimulation or feed ratio adjustments. Leveraging these attributes, the developed material introduces novel opportunities for light-writing applications, advanced information encryption, UV-sensing wearable devices, and insights into designing multifunctional intelligent materials for the future.

1. Introduction

Photo-stimuli-responsive smart materials have garnered significant attention for their fascinating color changes in fluorescence emission and absorption variations in response to external stimuli. These materials find wide applications in sensing, photo-rewritable patterns,[1] UV sensors,[2] biological imaging,[3] and anti-counterfeiting.[4] Typically, the photoswitching ability is achieved through special molecules with light-triggered chemical structure conversions, such as diarylethene (DAE),[5] spiropyran (SP),[6] azobenzene (AZO),[7] and redox photo-responsive components.[8] Among these, SP stands out for its transformation from a colorless non-fluorescent closed-ring structure to a purple-red fluorescent open-ring merocyanine (MC) isomer under UV irradiation, easily reversible by visible light treatment.[9] However, many spiropyran-based photo-switching materials only exhibit a single fluorescence peak upon UV or visible light exposure,[9a,10] making it challenging to observe luminescence when in the switched-off state. Thus, the development of materials with multiple emission centers, where one emission turns on while the other turns off or remains unchanged upon light irradiation, holds great promise for achieving enhanced stimulus response performance.

Lanthanide complexes are highly regarded for their exceptional photoluminescence (PL) characteristics, such as large Stokes shifts, narrow emission bands, high PL efficiency, long lifetimes, and multicolor emission.[11] Despite these advantages, lanthanide complexes are often in a powder state, posing challenges for further processing. To address this limitation, lanthanide metallopolymers have emerged as a promising alternative. These materials offer benefits like good processability, easy functional integration, enhanced structural stability, and adjustable architectural properties.[12] However, one significant drawback of metallopolymer materials is their susceptibility to damage and fracture during use, emphasizing the importance of incorporating self-healing capabilities. Fortunately, the coordination bonds between Ln^{3+} ions and ligands, coupled with hydrogen bonding within the polymer chains, hold promise for imparting self-healing properties to the desired PL materials. This dynamic nature enables autonomous repair of physical damage, restoration of original functions, prolonged lifespan, reduced maintenance costs, and waste prevention.[13] The integration of

D. Zhao, L. Guo, Q. Li, C. Yue, H. Li
School of Chemical Engineering and Technology
Hebei University of Technology
GuangRong Dao 8, Hongqiao District, Tianjin 300130, P. R. China
E-mail: lihuanrong@hebut.edu.cn

B. Han
Department of Orthodontics
Peking University School and Hospital of Stomatology
Beijing 100081, P. R. China
E-mail: kqbinghan@bjmu.edu.cn

K. Liu
Engineering Research Center of Advanced Rare Earth Materials
(Ministry of Education), Department of Chemistry
Tsinghua University
Beijing 100084, P. R. China
E-mail: kailiu@tsinghua.edu.cn

The ORCID identification number(s) for the author(s) of this article can be found under https://doi.org/10.1002/adma.202405164

DOI: 10.1002/adma.202405164

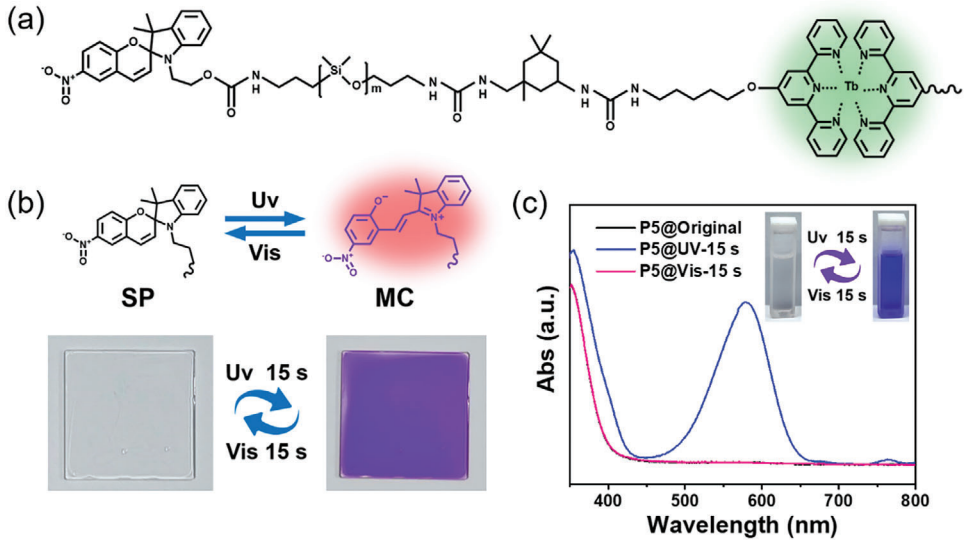

Figure 1. Chemical structure and design concept of photoPU polymers. a) Chemical structure illustration of the photo-stimuli-responsive samples. b) Digital images and (c) UV–vis absorption spectra of photo-stimuli-responsive behavior of the representative sample P5 (black line (SP state): original; blue line (MC state): exposure to 365 nm UV light 15 s; red line (MC state): recovered by visible light treatment).

superior PL performance, photoswitching ability, processing flexibility, and self-healing properties in this multifunctional intelligent material might open up new avenues for innovation. Although there are currently no reports on these aspects, we anticipate that such advancements will unlock exciting possibilities in material science.

Here, dual-emitting photoluminescent lanthanide metallopolymers, denoted as photoPU, are synthesized by cross-linking terpyridine (Tpy) and spiropyran (SP) functionalized polyurethanes through Tpy-Tb coordination bonds and hydrogen bonding among the polymer chains. By adjusting the SP/Tpy-Tb feed ratios (refer to Table S1, Supporting Information), a range of photo-stimuli-responsive metallopolymers exhibiting captivating color transformations post-365 nm UV exposure is developed. These alterations include switching from non-luminescent to red emission, green emission to red emission, green emission to yellow emission, and retaining green emission, along with distinct color changes from colorless to purple. Reversing transformations can be achieved upon subsequent treatment with visible light. The resulting photoPU materials demonstrate excellent processability, enabling coating on diverse substrates like glass, paper, and metal. They can also be formed into films using the solvent evaporation method and easily shaped into various desired forms. Moreover, the photoPU exhibits transparency in the SP state, satisfactory mechanical properties, and prompt room-temperature self-healing capabilities, enhancing their potential for practical applications significantly.[14]

2. Results and Discussion

2.1. Materials Design and Synthesis of Photochromic Metallopolymers

The key design concept of the self-healing photochromic polymers is to introduce both the photo-stimuli-responsive spiropyrans component and the luminescent Tpy-Tb segment into polydimethylsiloxane-based (PDMS-based) self-healing polymer chains (**Figure 1a**). Wherein, spiropyran derivatives can be covalently incorporated into PDMS-based polymer materials as a UV-sensing segment while maintaining their conformational freedom and photo-stimuli-responsive properties. The obtained photoPU polymers containing ring-closed spiropyran form (SP) are transparent, colorless, and non-fluorescent. When photoPU polymers were exposed to 365 nm UV light for only 15 s, spiropyran components can transform to a ring-opened merocyanine state (MC), resulting in a highly purple colored (visual color under daylight, see Figure 1b) and strong red fluorescence. The color change can be proved by their UV–vis absorption spectra. As shown in Figure 1c, the absorption spectra of the photoPU material exhibit a significant absorption peak centered at 578 nm after 15 s of exposure to 365 nm UV light, further treatment by visible light can quickly restore their original state. In addition, there are two other important design criteria: i) Minimize the feeding of expensive reagents Tpy, Tb^{3+}, and spiropyran while satisfying the demand for stimulus-response and luminescence capabilities. Therefore, the spiropyran and Tpy in the representative samples are 0.5% and 4% of the mass of PDMS, respectively (note that: the molar ratio of Tpy to Tb^{3+} is always 2:1); ii) Because the MC state of spiropyran show bright red-emission under UV light, we selected Tb^{3+} that can emit green light to coordinate with Tpy to obtain more elegant adjustment in luminescent color. According to our designed synthesis route, a series of photoPU products were prepared successfully (Figure S1, Supporting Information). We selected the Tb-contained material P5 as the representative sample due to its superior multi-color photoluminescence capability under specific conditions, which we will discuss later. The successful synthesis of the P5 can be demonstrated by Fourier transform infrared (FT-IR) (Figure S2, Supporting Information) and gel permeation chromatography (GPC) measurements (Figure S3, Supporting Information). The

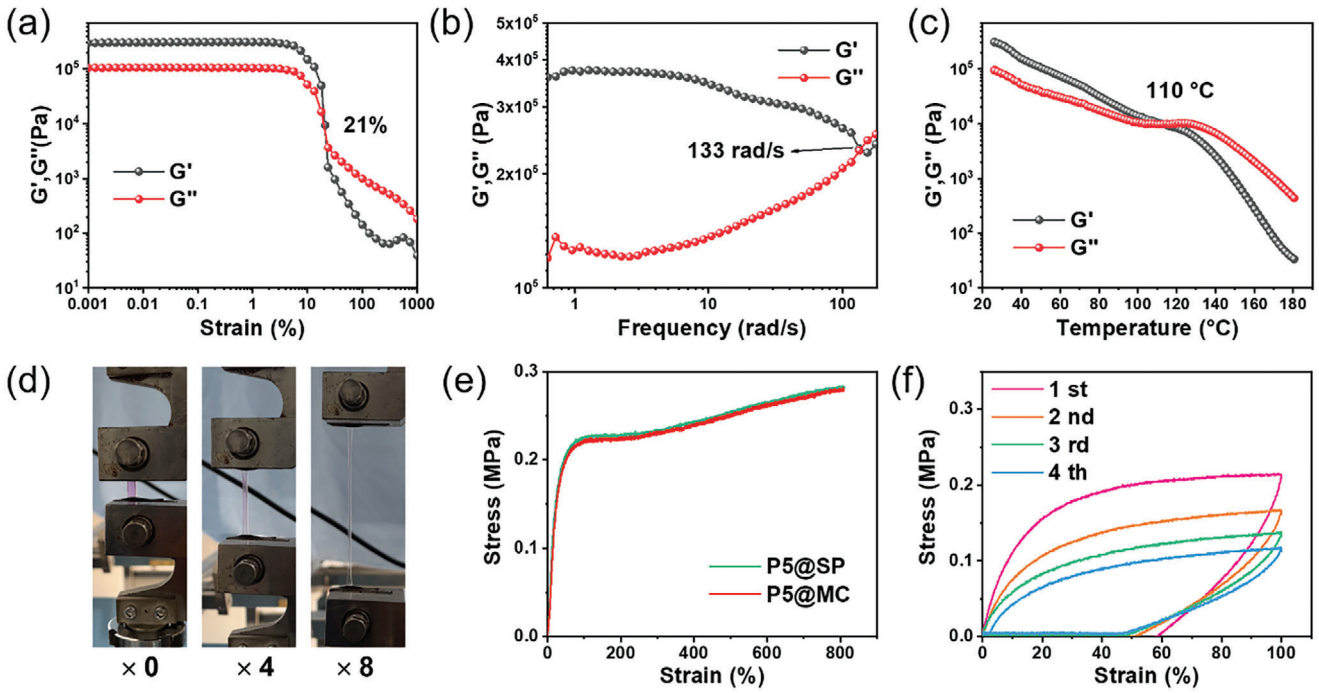

Figure 2. Viscoelasticity and mechanical properties of photoPU polymers. Rheological performances measurements, a) strain sweeps curve was tested with a strain of 0.001-1000% (frequency:1 Hz, temperature: 25 °C); b) frequency sweeps were tested from 0.068 to 628 rad s^{-1} (strain:1%, temperature: 25 °C); c) temperature dependence of storage modulus (G′) and loss modulus (G″) was tested from 25 °C to 180 °C (strain: 3%, frequency:1 Hz); b) Stretching digital photos, c) stress-strain curves and (d) loading and unloading curves to 100% strain of P5.

resulting P5 samples show low T_g (below −80 °C, see Figure S4, Supporting Information) and good thermal stability with an initial decomposition temperature of 218 °C (Figure S5, Supporting Information).

2.2. Mechanical Properties of Photosensitive Metallopolymers

First, rheological testing and tensile measurements were carried out to evaluate the viscoelasticity and mechanical properties of P5. At low strain amplitudes before 21% and small frequency (<133 rad s^{-1}), the response is solid-like (G′ > G″), until the yield point is reached where the G′ decreases and materials start to flow (**Figure** 2a,b). P5 did not show obvious thermally induced phase transitions before heating to 110 °C (Figure 2c). The above phenomena indicate that P5 possesses a solid-state response behavior different from the raw material liquid PDMS and a viscoelasticity similar to typical cross-linked polymers, thereby further proving the successful preparation of typical cross-linked metallopolymers.[15] The stress-strain tests show that both SP/MC states of P5 material exhibit similar tensile curves. This phenomenon is due to the low content of SP in the material (<0.5%), which cannot generate a significant impact on their mechanical properties. Specifically, P5 exhibits a tensile strength of 0.26 MPa, toughness of 1.83 MJ $m^{-3,}$ and high extensibility of 809%, respectively (Figure 2b,c). This phenomenon indicates that our metallopolymers have good mechanical properties, which endow them with the ability to be used in various complex environments.[16] Significant hysteresis was obtained during the continuous loading and unloading tensile tests, indicating the presence of energy dissipation, which is ascribed to the dissociation/recombination of dynamic crosslinking bonds that cannot be fully restored to their original state at a single cyclic scale (Figure 2d).[17] The energy dissipation gradually decreases from the 1st to 4th cycles (Table S2, Supporting Information), which is the famous Mullins effect, due to the increase of the volume fraction of the soft segment.[18] The above phenomena indicate that the resulting P5 is similar to the typical reported elastomers and features viscoelastic behavior.[13a,19]

2.3. Self-Healing and Recycling Abilities

Next, the self-healing abilities and recyclability of the synthesized photosensitive metallopolymers were studied. As shown in **Figure** 3a and Video S1 (Supporting Information), the fractured P5 sample can achieve self-healing and withstand its own weight after the cut surface is contacted for 16 s. To further investigate the self-healing capacity of the photochromic polymers, P5 samples were bisected and allowed to resplice at room temperature for varying periods and stretched until they broke again. As expected, the mechanical properties (stress, stain, and toughness) of the self-healed samples increase along with the prolongation of self-healing time (Figure 3b; Figure S6 and Table S3, Supporting Information). After 24 h of self-healing at room temperature, the tensile curve of the respliced sample can basically coincide with the original one, achieving a 100% self-healing efficiency, where the self-healing efficiency is defined as the ratio of the toughness after self-healing to the initial one. Furthermore, the obtained photoPU can be easily dissolved into dichloromethane

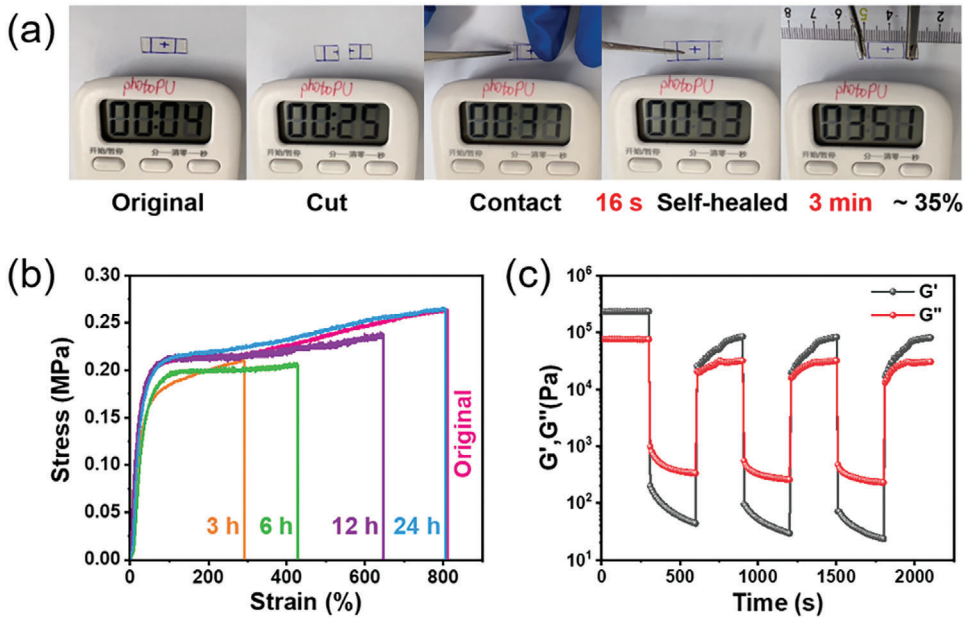

Figure 3. Self-healing abilities of photoPU polymers. a) Self-healing behavior images and (b) tensile stress-strain curves of fractured photochromic P5 polymers self-healed for different times. c) Alternate step strain rheological measurement of storage modulus (G′) and loss modulus (G″) of P5.

(DCM) solvents (even without stirring), and then be re-casted and dried to obtain recycled samples. The photosensitivity and mechanical properties of the recovered samples are maintained (Figure S7, Supporting Information). The self-healing and recycling abilities of the prepared P5 originate from the dynamic nature of hydrogen bonding and Tpy-Tb coordination interactions, which can be verified via rheological experiments.[20] As shown in Figure 3c, the elastomer can transfer from solid state (G′ > G″) at 0.1% shear strain to liquid state (G′ < G″) at 100% strain owing to the breaking of the dynamic networks. After the strain recovers to 0.1%, the fractured dynamic bonds are reconstructed and the polymer network is restored to the solid-state again (G′ > G″). Also, the product can rapidly alternate between the two states.[21] Furthermore, the non-crystallized loose structure (Figure S8, Supporting Information) and low Tg (below −80 °C, see Figure S4, Supporting Information) endow the P5 polymer chains with diffusion and mobility capabilities, which could also promote self-healing.[22]

2.4. Photoluminescent and Photo-Stimuli-Responsive Performance

We then explored the photoluminescent (PL) properties and photo-stimuli-responsive performance in response to external light stimuli of a series of obtained materials. Fixing the feed of spiropyran at 0.5 mg and adjusting the feed of Tpy to 0.5, 1, 2, 4, 8 mg, respectively (the specific feed ratios are summarized in Table S1, Supporting Information), a series of variable photosensitive materials were prepared (note that: the molar ratio of Tpy to Tb^{3+} is always 2:1). As shown in **Figure** 4a, along with the increasing of the Tpy-Tb contents, fascinating color changes in emission phenomena were obtained after 15 s 365 nm UV radiation, including non-luminescent to red-emission (P2 and P3 under 302 and 365 nm UV light), weak green-emission to red-emission (P4 under 302 nm UV light), green-emission to yellow-emission (P5 under 302 nm UV light), green-emission retention (P6 under 302 nm UV light), and blue-emission to red-emission (P4, P5, P6 under 365 nm UV light). Meanwhile, the visual colors of the materials under daylight switch from colorless and transparent to deep purple (Figure 1b). Compared with the currently reported photosensitive materials, our lanthanide (Ln) metallopolymers show advantages of fast response (<15s), a wide range of luminescent color switching, along distinct color transformation (colorless to purple) ability.[23]

Subsequently, the Tb-contained sample P5 was selected as the representative sample, since P5 can display the four luminescent colors under specific conditions, this is more numerous than other samples. In the initial state, the P5 sample is a transparent and colorless polymer film under daylight (Figure 4d), with obvious green-emission (attributed to Tpy-Tb) under 302 nm UV light and blue-emission (attributed to Tpy ligands itself) at 365 nm UV light (Figure 4a). After 15 s of exposure to a 365 nm UV light, the material rapidly transformed into a deep purple color due to the transition of spiropyran from a ring-closed state (SP) to the ring-open merocyanine form (MC) (see Video S2, Supporting Information). Meanwhile, due to the addition of a small amount of red-emission caused by MC, the luminescent color changed from green to a clear yellow-emission under 302 nm UV light.[24] However, due to the sufficient degrees of freedom of the spiropyran component in the material, spiropyran has transitioned from a closed-ring state (SP) to an open-ring state (MC) and emitted the corresponding red light, when tested in the Edinburgh Instruments FS920P spectrometer. Therefore, we were unable to obtain the fluorescence spectrum of the initial state of the sample and only obtained a series of fluorescence curves after exposure to UV radiation.

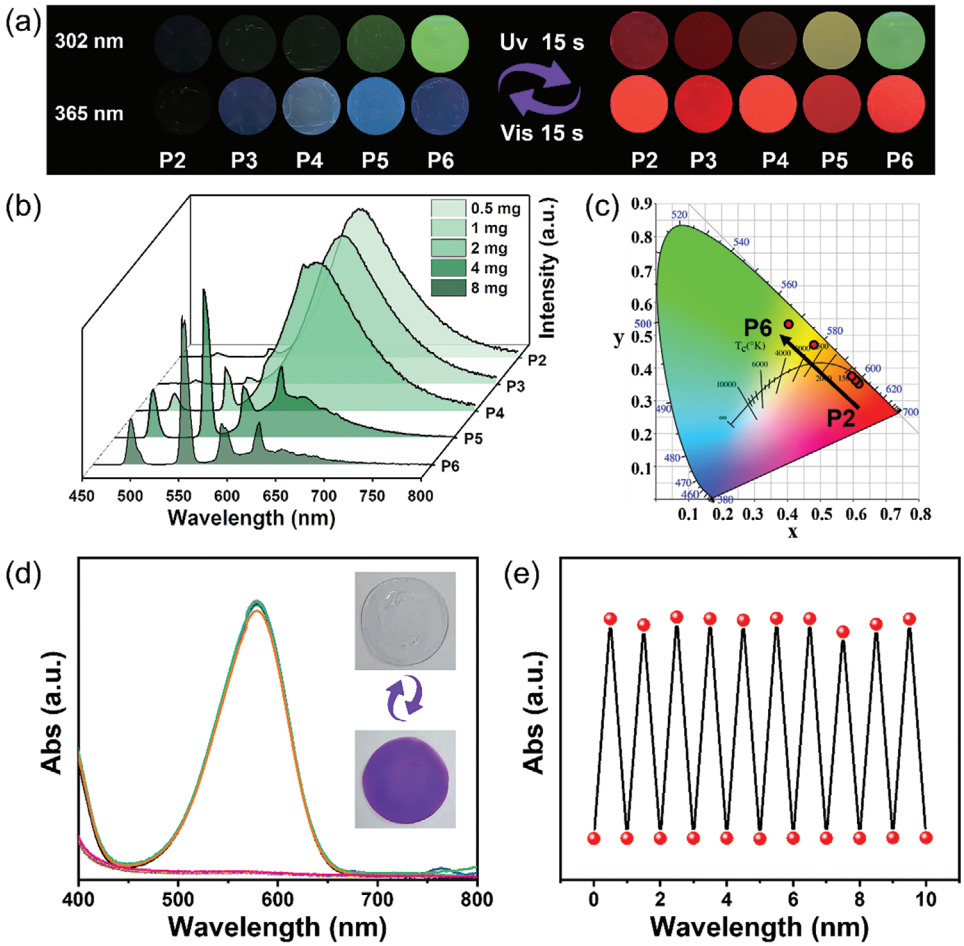

Figure 4. Photoluminescent and photo-stimuli-responsive performance of photoPU materials. a) Digital images of a series of Tb^{3+}-containing polymers. From left to right: the feed of SP is kept at 0.5 mg, accompanied by a gradual increase in Tpy content from 0.5, 1, 2, 4, and 8 mg, respectively, the molar ratio of Tpy to Tb^{3+} is 2:1, the obtained samples are noted as P2, P3, P4, P5, and P6, respectively. b) Photoluminescence (PL) spectra excited at 300 nm and monitored at 544 nm of materials P2 to P6 (MC-state), and c) their corresponding emission colors in the CIE 1931 diagrams. d) UV–vis absorption spectra (inset digital image belonging to P5 film) and e) absorption intensity at 578 nm of representative sample P5 during cyclic exposure to UV/vis radiation (solvent: DCM; concentration: 10^{-4} mol L^{-1}).

The excitation spectrum of P1 (sample with spiropyran and without Tpy-Tb component) shows a broadband absorption in the range 250 to 450 nm centered at 379 nm, and its fluorescence spectrum excited at 300 nm displays a broadband emission peak centered at 640 nm, which produces the red-emission behavior (Figure S9, Supporting Information). The excitation spectrum of P5 (sample containing both spiropyran and Tpy-Tb simultaneously) shows a broadband absorption in range 225 to 360 nm centered at 323 nm (Figure S10, Supporting Information), and its emission spectrum excited at 300 nm shows emission peaks centered at 490, 542, 583, 622 nm, attributed $^5D_4 \rightarrow {}^7F_J$ (J = 6, 5, 4, 3) transitions, in which the peak at 542 nm generated by $^5D_4 \rightarrow {}^7F_5$ dominate green-emission (Figure S11, Supporting Information). Along with the adjustment of Tpy content from 0.5 to 8 mg (P2 to P6), the excitation spectra relative intensity at 323 nm (monitored at 544 nm) gradually increases (Figure S10, Supporting Information). Meanwhile, the emission spectra of the P2 to P6 samples excited at 300 nm exhibit increased characteristic peaks of Tb^{3+} at 542 nm (Figure 4b), and the emission color gradually changes from red through yellow to green (Figure 4a), consistent with the emission colors in the CIE 1931 diagrams (Figure 4c). In addition, Eu^{3+} ions that can emit red light can be added to the luminescent photochromic material to achieve multiple regulations of luminescent colors (Figure S12, Supporting Information). Furthermore, our products have good fatigue resistance, even after 10 cycles of vis/UV light stimulation, their stimulus-response ability is still maintained (Figure 4d,e).

2.5. Light-Writing and Information Encryption Properties

After achieving a colorless-to-purple color change caused by 365 nm UV light, non-contact UV light (365 nm) and visible light could be used as the "pen" to further explore real-time light-writing display of transient information. Due to the fast and reversible form transition of the spiropyran in the photoPU film, this light-writing mode was proved to be real-time, enabling the reversible display of arbitrary hand-written information. By

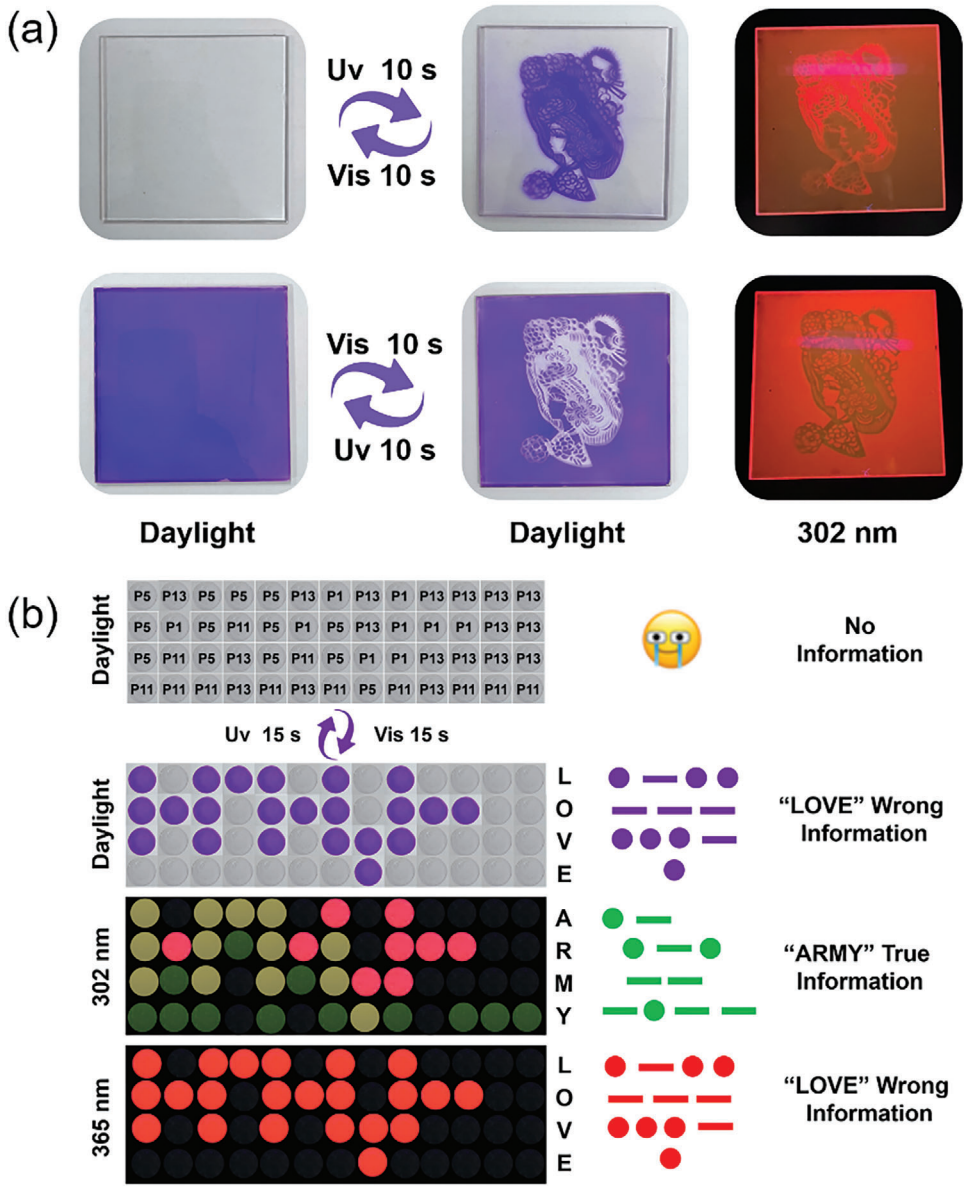

Figure 5. Light-writing and information encryption properties of photoPU materials. a) Light-writing behavior on photoPU material (8 cm × 8 cm). b) Morse-coded muti-color microarray for information encryption. The numbers in the first image represent the identifier of each pixel sample, as detailed in Table S1 (Supporting Information).

combining the light-writing ability of our materials with traditional Chinese Paper Cuttings, we can easily obtain the corresponding portraits of opera characters (**Figure 5**a). Also, due to the good fatigue resistance of the photo-stimuli-responsive ability of the obtained photoPU, dynamic information "HEBUT" could be easily written on the same rewritable platform (Figure S13, Supporting Information).

In addition, our materials photoPU show broad application prospects in the field of information anti-counterfeiting due to their ability to simultaneously change color (absorption) and fluorescence (emission) in response to external photo stimuli. However, traditional luminescent encryption materials are often easily identifiable and cannot satisfy practical demand. Therefore, it is necessary to develop high-level multiple encryption protection for information. We believe that the prepared photo-stimuli-responsive smart materials photoPU has broad practical significance in the advanced anti-counterfeiting field, due to their complex color changes in fluorescence (emission) and distinct color (absorption) variations under external photo stimuli.

Morse code is a magical cipher, which is a signal composed of dots and dashes, and can express different English letters by the different arrangement order of dots and dashes. In consideration of the multi-color emission output of the photoPU products, information can be encrypted and transmitted by combining the Morse code with the photo-stimulus-response ability of our sample, in which a single sample and three consecutive

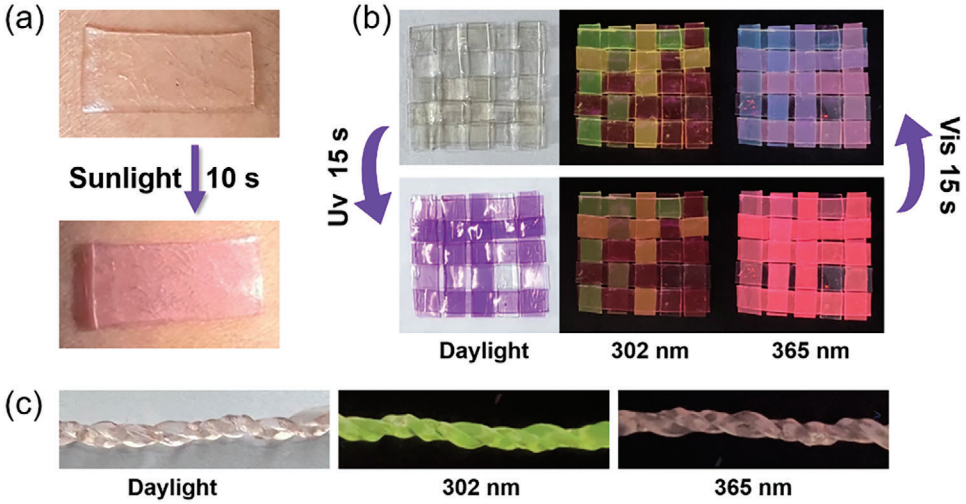

Figure 6. Potential applications of photoPU elastomers for UV-sensing and wearable devices. a) Skin-mounted UV detection patch, b) multicolor photosensitive sample bar (P5, P6, P8, and P0) weave arrays and (c) luminesce images of luminescent twisted ropes based on PhotoPU elastomers.

sample points represent "dots" and "dashes", respectively. As shown in Figure 5b, we only obtained 4 × 13 transparent sample arrays, there is no information available initially under daylight. Subsequently, after exposure to 365 nm UV light for only 15 s, the information "LOVE" can be easily detected under daylight by decrypting the Moss codes. However, information "LOVE" is set as false information. The correct information "ARMY" can only be obtained under a 302 nm UV light, while false information "LOVE" can also be obtained under a 365 nm UV light. The sample information arrays can be restored to their original state again by exposure to visible light for 15 s. Among the above-mentioned pixel samples, there is also a process of color change in the luminescence of our samples (please refer to Figure 4d; Figure S14 (Supporting Information) for specific details), which also plays a role in anti-counterfeiting. In addition, our encrypted information array can be rearranged and combined to express different information, similar to "Movable Type Printing", a great invention of ancient China, which undoubtedly has significance in material reuse and energy conservation (Figure S15, Supporting Information).

2.6. PhotoPU for UV-Sensing and Wearable Devices

As is well known, the UV light in sunlight can be mainly divided into UVA (λ_{max} = 368 nm), UVB (λ_{max} = 306 nm), and UVC (λ_{max} = 265 nm) radiation, where UVB and UVC can be absorbed by the ozone layer ≈98% and most of UVA can reach the earth's ground. UVA radiation, also known as the "tanning section", has strong penetration into clothing and human skin, reaching deep into the dermis and causing melanin deposition, blackening the skin, leading to skin aging and severe damage.[25] To characterize the response to UV radiation, we tested the color change of P5 elastomer after exposure to 254, 302, and 365 nm for 15 s, respectively. Our material is most sensitive to 365 nm UV light, equivalent to UVA radiation in sunlight (Figure S16, Supporting Information). As shown in **Figure 6a**, the UV detection film attached to the skin quickly changes from colorless to light purple under sunlight exposure for only 10 s, further placement of the purple sample under indoor lighting for 5 min can restore its original transparent and colorless state. Superior repeatability is achieved, even after 6 cycles (Figure S17, Supporting Information).

Compared with the currently reported powder photosensitive materials,[26] our metallopolymers have better processing performance. The obtained photoPU materials have excellent processability, which can be coated on the surface of substrates such as glass (Figure S18, Supporting Information), paper (Figure S19, Supporting Information), and metal (Figure S20, Supporting Information), and can be prepared into films by solvent evaporation method and easily cut into various desired shapes. We can weave different numbered material strips together, achieving multiple functions such as aesthetics, anti-counterfeiting, UV detection, luminescence, and self-healing simultaneously (Figure 6b). Besides, uniform twirling elastic ropes can be prepared by weaving multiple photoPU sample strips (Figure 6c), especially by weaving fluorescent stripes of different colors together to visualize the texture structure of the elastic rope (Figure S21, Supporting Information). The above results indicate that our materials have great application prospects in UV-sensing wearable devices.

3. Conclusion

Visible and ultraviolet light-driven photo-stimuli-responsive luminescent elastomers with commendable mechanical properties and self-healing capabilities were successfully developed by incorporating spiropyran and Tpy-Ln components into a unified polymer structure. The preserved stimulus-response functionality of spiropyran, even after covalent bonding to PDMS-based polymer chains, imparts rapid photo-response (<15 s) and captivating color variations in emission (fluorochromic attributes) and absorption (photochromic property) to the products. By adjusting the proportions of each raw material, precise control over the stimulus-response and luminescent color can be achieved. Furthermore, the resultant photoPU materials exhibit exceptional processability, lightweight nature, fatigue

resistance, transparency, colorlessness, acceptable mechanical properties, and quick room-temperature self-healing characteristics. This groundbreaking study not only opens up novel avenues in advanced applications such as information encryption, anti-counterfeiting measures, photo-rewriting, and wearable UV sensors but also offers valuable insights for developing the next generation of photo-stimuli-responsive luminescent materials.

Supporting Information

Supporting Information is available from the Wiley Online Library or from the author.

Acknowledgements

This work was supported by the National Natural Science Foundation of China (22175053, 22125701, 22388101, and 22020102003), the Tianjin Natural Science Foundation (23JCZDJC00500) and the Government Guide the Development of Local Science and Technology Special Funds (236Z1202G, 206Z1401G).

Conflict of Interest

The authors declare no conflict of interest.

Data Availability Statement

The data that support the findings of this study are available from the corresponding author upon reasonable request.

Keywords

lanthanide, photoluminescence, photosensitive, self-healing, spiropyran

Received: April 10, 2024
Revised: June 13, 2024
Published online:

[1] A. Julià-López, D. Ruiz-Molina, J. Hernando, C. Roscini, *ACS Appl. Mater. Interfaces* **2019**, *11*, 11884.
[2] Z. Ke, K. Chen, Z. Li, J. Huang, Z. Yao, W. Dai, X. Wang, C. Liu, S. Xiang, Z. Zhang, *Chin. Chem. Lett.* **2021**, *32*, 3109.
[3] a) L. Zhu, W. Wu, M.-Q. Zhu, J. J. Han, J. K. Hurst, A. D. Li, *J. Am. Chem. Soc.* **2007**, *129*, 3524; b) J. Sobhanan, A. Anas, V. Biju, *Chem. Rec.* **2023**, *23*, 202200253.
[4] a) C. Li, J. Liu, X. Qiu, X. Yang, X. Huang, X. Zhang, *Angew. Chem.* **2023**, *135*, 202313971; b) A. Abdollahi, B. Ghasemi, S. Nikzaban, N. Sardari, S. Jorjeisi, A. Dashti, *ACS Appl. Mater. Interfaces* **2023**, *15*, 7466.
[5] a) M. Li, W.-H. Zhu, *Acc. Chem. Res.* **2022**, *55*, 3136; b) L. Hou, R. Ringström, A. B. Maurer, M. Abrahamsson, J. Andréasson, B. Albinsson, *J. Am. Chem. Soc.* **2022**, *144*, 17758.
[6] a) J. Tang, Y. Tian, Z. Lin, C.-H. Zhang, P. Zhang, R. Zeng, S. Wu, X. Chen, J. Chen, *ACS App. Mater. Interfaces* **2022**, *15*, 2237; b) S. Bhattacharyya, M. Maity, A. Chowdhury, M. L. Saha, S. K. Panja, P. J. Stang, P. S. Mukherjee, *Inorg. Chem.* **2020**, *59*, 2083.
[7] a) Y. Li, B. Xue, J. Yang, J. Jiang, J. Liu, Y. Zhou, J. Zhang, M. Wu, Y. Yuan, Z. Zhu, *Nat. Chem.* **2023**, *16*, 446; b) C. Van Dyck, S. Osella, D. Cornil, J. Cornil, *ACS Appl. Mater. Interfaces* **2021**, *13*, 27737.
[8] a) T. Yimyai, D. Crespy, A. Pena-Francesch, *Adv. Funct. Mater.* **2023**, *33*, 2213717; b) J. Wan, J. Xu, S. Zhu, J. Li, G. Ying, K. Chen, *J. Cleaner Prod.* **2023**, *419*, 138281.
[9] a) D. Euchler, C. R. Ehgartner, N. Hüsing, A. Feinle, *ACS Appl. Mater. Interfaces* **2020**, *12*, 47754; b) T. Yang, Y. Zuo, S. Feng, *Mater. Des.* **2021**, *207*, 109867.
[10] J. Allouche, A. Le Beulze, J.-C. Dupin, J.-B. Ledeuil, S. Blanc, D. Gonbeau, *J. Mater. Chem.* **2010**, *20*, 9370.
[11] a) D. Zhao, Q. Li, L. Guo, C. Yue, J. Yang, Y. Wang, H. Li, *Chem. Eng. J.* **2023**, *468*, 143418; b) Y. Wang, Y. Liu, G. Xie, J. Chen, P. Li, Y. Zhang, H. Li, *ACS Appl. Mater. Interfaces* **2022**, *14*, 5951.
[12] a) T. Sato, M. Higuchi, *Chem. Commun.* **2012**, *48*, 4947; b) D. Zhao, J. Yang, X. Tian, J. Wei, Q. Li, Y. Wang, *Chem. Eng. J.* **2022**, *434*, 134806; c) K. Y. Zhang, S. Liu, Q. Zhao, W. Huang, *Coord. Chem. Rev.* **2016**, *319*, 180; d) S. Goetz, S. Zechel, M. D. Hager, G. R. Newkome, U. S. Schubert, *Prog. Polym. Sci.* **2021**, *119*, 101428.
[13] a) X. Wang, J. Xu, Y. Zhang, T. Wang, Q. Wang, S. Li, Z. Yang, X. Zhang, *Nat. Commun.* **2023**, *14*, 4712; b) C. H. Li, J. L. Zuo, *Adv. Mater.* **2020**, *32*, 1903762.
[14] a) Y. Xie, M. C. Arno, J. T. Husband, M. Torrent-Sucarrat, R. K. O'Reilly, *Nat. Commun.* **2020**, *11*, 2460; b) Y. Xie, G. Sun, J. Li, L. Sun, *Adv. Funct. Mater.* **2023**, *33*, 2303663; c) M. Tao, X. Liang, J. Guo, S. Zheng, Q. Qi, Z. Cao, Y. Mi, Z. Zhao, *ACS Appl. Mater. Interfaces* **2021**, *13*, 33574.
[15] a) H. Xu, J. Tu, H. Li, J. Ji, L. Liang, J. Tian, X. Guo, *Chem. Eng. J.* **2023**, *454*, 140101; b) C.-H. Li, C. Wang, C. Keplinger, J.-L. Zuo, L. Jin, Y. Sun, P. Zheng, Y. Cao, F. Lissel, C. Linder, *Nat. Chem.* **2016**, *8*, 618.
[16] a) Y. Wan, X.-C. Li, J. Chen, Q. Wang, C. Liu, C.-F. Liu, W.-Y. Lai, *Macromolecules* **2023**, *56*, 3345; b) L. Jiang, J. Li, N. Peng, M. Gao, D.-Y. Fu, S. Zhao, G. Li, *Polymer* **2022**, *263*, 125509.
[17] a) R. Guo, Q. Zhang, Y. Wu, H. Chen, Y. Liu, J. Wang, X. Duan, Q. Chen, Z. Ge, Y. Zhang, *Adv. Mater.* **2023**, *35*, 2212130; b) X. Hou, B. Huang, L. Zhou, S. Liu, J. Kong, C. He, *Adv. Mater.* **2023**, *35*, 2301532.
[18] J. Yang, Z. Zhang, Y. Yan, S. Liu, Z. Li, Y. Wang, H. Li, *ACS Appl. Mater. Interfaces* **2020**, *12*, 13239.
[19] P. Hu, Y. Zhang, S. Zhou, T. Chen, D. Wang, T. Liu, Y. Wang, J. Chen, Z. Wang, J. Xu, *Chem. Eng. J.* **2023**, *464*, 142543.
[20] F. Sun, J. Xu, T. Liu, F. Li, Y. Poo, Y. Zhang, R. Xiong, C. Huang, J. Fu, *Mater. Horiz.* **2021**, *8*, 3356.
[21] a) X. Liu, Y. Li, X. Fang, Z. Zhang, S. Li, J. Sun, *ACS Mater. Lett.* **2022**, *4*, 554; b) M. Martínez-Calvo, O. Kotova, M. E. Möbius, A. P. Bell, T. McCabe, J. J. Boland, T. Gunnlaugsson, *J. Am. Chem. Soc.* **2015**, *137*, 1983.
[22] P. Qu, C. Lv, Y. Qi, L. Bai, J. Zheng, *ACS Appl. Mater. Interfaces* **2021**, *13*, 9043.
[23] a) Y. Li, Y. Yang, X. Guo, Y. Chen, Z. Wang, L. Hu, W. Wu, J. Zhu, *ACS Appl. Nano Mater.* **2023**, *6*, 5817; b) X. Li, H. Wang, J. Chen, Y. Tian, C. Xiang, W. Liu, Z. Zhou, J. Cui, X. Chen, *Adv. Funct. Mater.* **2023**, *33*, 2303765.
[24] R. Klajn, *Chem. Soc. Rev.* **2014**, *43*, 148.
[25] M. E. Lee, A. M. Armani, *ACS Sens.* **2016**, *1*, 1251.
[26] R. Yang, X. Ren, L. Mei, G. Pan, X. Z. Li, Z. Wu, S. Zhang, W. Ma, W. Yu, H. H. Fang, *Angew. Chem., Int. Ed.* **2022**, *61*, 202117158.